RADIOCARBON, Vol 52, Nr 1, 2010, p 129–147 © 2010 by the Arizona Board of Regents on behalf of the University of Arizona

RECONSTRUCTION OF 130-KYR RELATIVE GEOMAGNETIC INTENSITIES FROM ^{10}Be IN TWO CHINESE LOESS SECTIONS

Weijian Zhou[1,2,3] • Feng Xian[1,2] • J Warren Beck[4] • A J Timothy Jull[4] • Zhisheng An[1] • Zhenkun Wu[1,2] • Min Liu[2] • Maobai Chen[1,2] • Alfred Priller[5] • Walter Kutschera[5] • George S Burr[4] • Huagui Yu[1,6] • Shaohua Song[1] • Peng Cheng[1,2] • Xianghui Kong[1,6]

ABSTRACT. Efforts to extract weak geomagnetic excursion signals from Chinese loess-paleosol ^{10}Be have generally been unsuccessful due to the complexities of its accumulation, because the geomagnetic and climate (precipitation and dust) signals contained in loess-paleosol sequence are tightly overprinted. Here, we present a reconstruction of geomagnetic relative paleointensities for the past 130 kyr from ^{10}Be records in 2 Chinese loess-paleosol sections using a correction based on the correlation of ^{10}Be with magnetic susceptibility (SUS) to remove the climatic contamination. Both these records reveal the Laschamp and Blake events, which lie in the loess and paleosol (L_1SS_1 and S_1SS_3) horizons corresponding to mid-MIS 3 and 5e, respectively. The good agreement between our results and other geomagnetic intensities reconstructions from Atlantic and Pacific sediments indicates that our method is robust. Our study suggests the potential application of loess-paleosol ^{10}Be for reconstructing geomagnetic intensity variations spanning the whole Quaternary.

INTRODUCTION

The cosmogenic radionuclide ^{10}Be is produced by cosmic-ray spallation in Earth's atmosphere. Its production rate there is regulated by the geomagnetic field intensity (e.g. Frank et al. 1997; Muscheler et al. 2005), so that its accumulated concentration in eolian sediments can in principal be used to derive high-resolution records of geomagnetic field changes. Chinese loess-paleosol sequences provide us with a good opportunity for such studies since they are a well-known archive for paleogeomagnetic and paleoclimatic studies with independent age constraints (An et al. 1990; Zhou et al. 1990; Zhu et al. 2007). However, there are few geomagnetic excursion studies from the Chinese loess-paleosol ^{10}Be record reported previously due to the complexities arising from 2 sources of ^{10}Be: one is related to the precipitation effect and the other to the incorporation of transported and recycled eolian dust (Shen et al. 1992; Beer et al. 1993; Heller et al. 1993; Gu et al. 1996). The geomagnetic excursions and reversals are important time markers for chronostratigraphic correlations, as systematic magnetostratigraphic studies have shown differences in short-lived excursions such as the Blake event observed in different loess-paleosol sequences (Evans and Heller 2001). Hence, it is necessary to develop an effective method for the reconstruction of geomagnetic field variations from the alternative loess ^{10}Be records by decoupling the climate and geomagnetic influences, to provide new cross-checking evidence.

We know that loess/paleosol magnetic susceptibility is largely due to secondary mineral formation, which in turn is controlled by soil moisture, which can be related to climate (Maher and Thompson 1988; Zhou et al. 1990). Inspired by the high similarity between measured ^{10}Be and magnetic susceptibility proxy in loess (Shen et al. 1992; Beer et al. 1993; Wu 2004), we first initiated the idea of separating the geomagnetic modulated ^{10}Be signal from the total ^{10}Be concentration, by taking loess susceptibility as a proxy for determining the ^{10}Be component affected by climate factors (dust-fall

[1]State Key Laboratory of Loess and Quaternary Geology, Institute of Earth Environment, Chinese Academy of Sciences, Xi'an 710075, China.
[2]Xi'an AMS Center, Xi'an 710052, China.
[3]Human Settlements and Engineering School of Xi'an Jiaotong University, Xi'an 710049, China. Corresponding author. Email: weijian@loess.llqg.ac.cn.
[4]NSF-Arizona AMS Facility, University of Arizona, Tucson, Arizona 85721, USA.
[5]VERA (Vienna Environmental Research Accelerator), University of Vienna, Waehringer Str. 17, Vienna 1090, Austria.
[6]Graduate University of Chinese Academy of Sciences, Beijing 100049, China.

https://doi.org/10.1017/S0033822200045082 Published online by Cambridge University Press

and wet precipitation), to reconstruct the paleomagnetic intensity (Zhou et al. 2007a). Three assumptions for such a separation need to be made. First, we assumed that the ^{10}Be concentration in dry dust is quasi-homogeneous in space with fairly constant values (Zhou et al. 2007a). Secondly, we assumed that the ^{10}Be inherited from dust is equal to that concentration found in loess during the driest period such as the last glacial maximum (LGM) when the precipitation was nearly negligible. Third, we assumed the functions can be separated arithmetically, as suggested by Zhou et al. (2007a,b). These approaches allowed us to approximately estimate the dust ^{10}Be background signals (An and Sun 1995; Xian et al. 2008).

In the following, we introduce a new method to reconstruct the past 130-kyr relative ^{10}Be production rates and geomagnetic intensities from 2 loess ^{10}Be records. We chose to analyze loess profiles from the Luochuan and Xifeng sections so that we could compare the time frame containing the Blake and Laschamp geomagnetic excursions. Even though these 2 sections are considered difficult for interpreting geomagnetic excursions due to differences in signal smoothing (e.g. Zhu et al. 1998; Pan et al. 2002), we chose them because each has well-established pre-existing sediment depth age models.

MATERIAL AND METHODS

Sampling and Proxies Measurements

Analyses were performed on the 1220-cm- and 1490-cm-length cores of Luochuan (35°45′N, 109°25′E) and Xifeng (35°42′N, 107°38′E) sections (Figure 1). Magnetic susceptibility was measured at 1-cm intervals as shown in Figure 2. ^{10}Be measurements for Luochuan were done at 4-cm intervals, except during the last glacial maximum (LGM), where measurements were done at 1-cm intervals. ^{10}Be measurements for Xifeng were made at 8–10 cm intervals, except during marine isotope stage 3 (MIS 3) and part of paleosol S_1, where it was sampled at 2–4 cm intervals. A total of 306 and 230 BeO samples from Luochuan and Xifeng, respectively, were chemically prepared in Xi'an, and measured in the Xi'an AMS Center, VERA in Vienna, and the NSF-Arizona AMS lab with a precision better than 3% (Zhou et al. 2007a). (See full results in Appendix, Tables 1 and 2.)

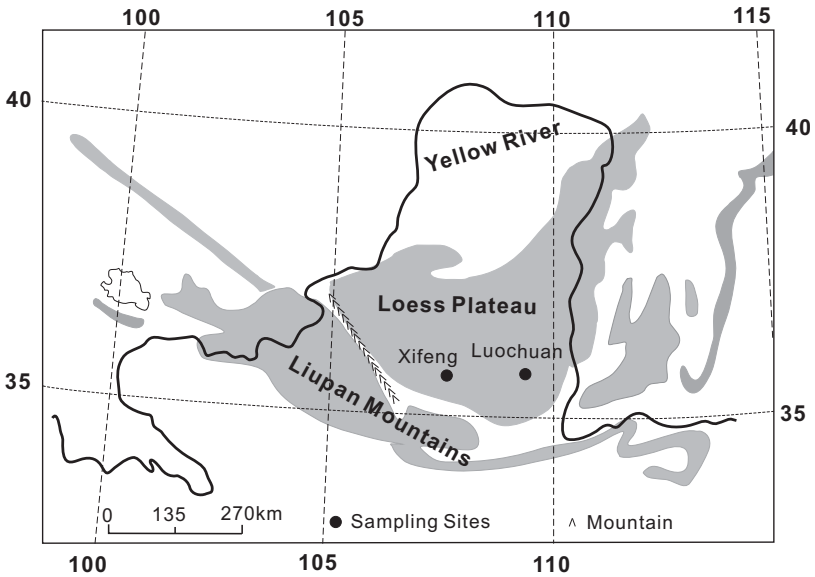

Figure 1 Map showing the Chinese Loess plateau (shaded areas), the Liupan Mountains, and the 2 sites for this study

https://doi.org/10.1017/S0033822200045082 Published online by Cambridge University Press

Timescales

The subdivisions of the paleosol S_1 unit are correlated to the oxygen isotope substages 5e–5a by An et al. (1991), so that chronologies of our 2 sections could be derived on the basis of the correlation between loess-paleosol magnetic susceptibility with the marine oxygen isotope (MIS). In each case, we assumed that the MIS 2/1, 5/4, and 6/5 transitions corresponded to the inferred L_1/S_0 (12.3 kyr BP), S_1/L_1 (79 ± 1 kyr BP) (Johnsen et al. 2001), and L_2/S_1 (129.8 ± 1 kyr BP) (Yuan et al. 2004), and used these as boundaries for age interpolation using a grain-size-based sediment accumulation rate model (Porter and An 1995). The Luochuan age scale was also cross-checked using a combination of optical luminescence (OSL) and ^{14}C ages (Figure 2b; Zhou et al. 2007a). The Xifeng section was carefully correlated to Luochuan and the Dongge-Hulu Cave $\delta^{18}O$ record (Wang et al. 2001; Yuan et al. 2004) for establishing a robust chronology over the past 130 kyr.

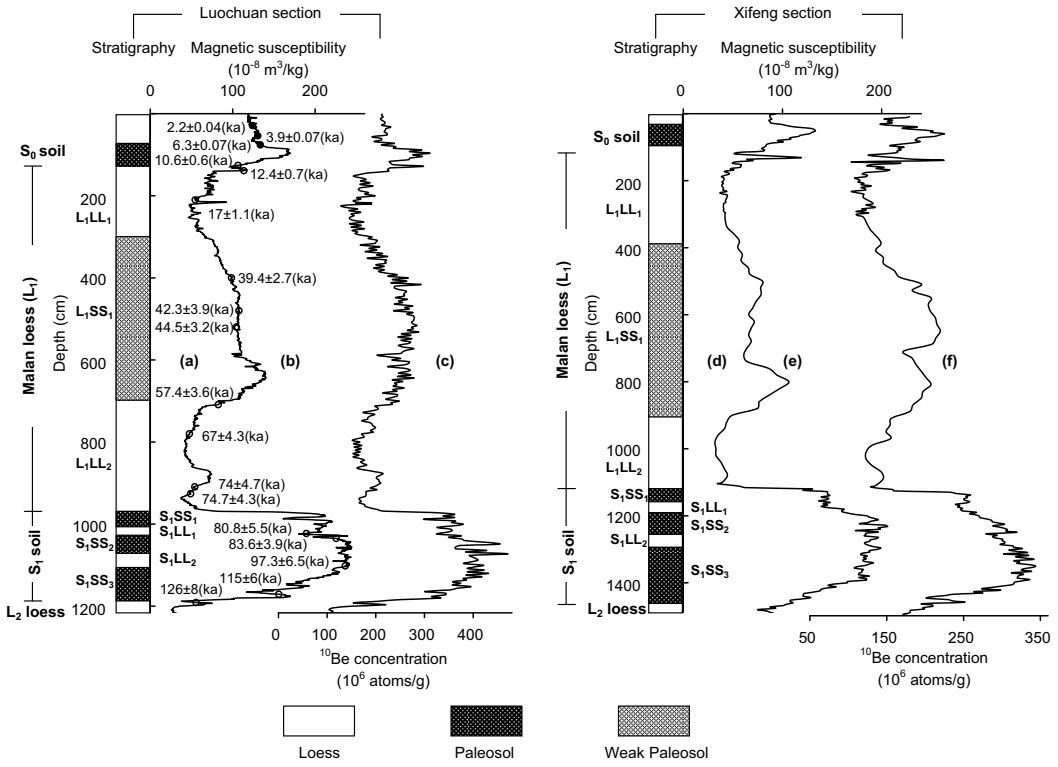

Figure 2 Stratigraphy, magnetic susceptibility, and ^{10}Be concentration of (a)-(c) Luochuan and (d)-(f) Xifeng sections. OSL (black circles) and ^{14}C (black dots) data are after Lu et al. (2007) and Zhou et al. (2007a), respectively. Typical strata such as Malan loess (L_1) and Last interglacial soil (S_1) are subdivided following Kukla and An (1989).

Similarity Between the Loess ^{10}Be and Magnetic Susceptibility

The loess-paleosol magnetic susceptibility is a function not only of eolian dust flux but also of pedogenic processes induced by precipitation, which controls soil moisture and the growth rate of pedogenic magnetic minerals (Maher and Thompson 1988; Kukla and An 1989; An et al. 1991; Maher et al. 1994; Porter et al. 2001). Porter et al. (2001) have concluded that other meteorological factors and grain-size effects on the pedogenic index appear to be insignificant. This is also similar for the loess-paleosol ^{10}Be record, as the local atmospheric fallout rate depends strongly on the wet

https://doi.org/10.1017/S0033822200045082 Published online by Cambridge University Press

precipitation (Beer et al. 1993; Heller et al. 1993; Zhou et al. 2007a). We know, however, that a fraction of the ^{10}Be concentration contained in loess-paleosols is derived from a dust source, but we believe that the same dust component bears both the recycled ^{10}Be and magnetic susceptibility components. Thus, both ^{10}Be and magnetic susceptibility in loess have signals containing a recycled dust component and a component that depends on the rainfall amount. The only difference is that the loess-paleosol ^{10}Be contains an additional signal arising from geomagnetic field variations (Zhou et al. 2007a). The high similarity ($r = 0.95$, Figure 2) between the loess ^{10}Be and magnetic susceptibility curves indicates both ^{10}Be and magnetic susceptibility are related to climate factors (precipitation and dust flux) in the same manner. Therefore, a linear regression between ^{10}Be and susceptibility can remove the climate-contributed ^{10}Be components and one can thus obtain the geomagnetic modulated ^{10}Be signals as suggested by Zhou et al. (2007b) based on an analysis that assumes that these 2 factors can be separated arithmetically and that the regression is linear. This assumption is clearly a significant approximation since the geomagnetic component may also have a component in the precipitation ^{10}Be.

Data Analysis Method

The main step of our analysis is first to extract the climate-contributed ^{10}Be from the Be(M), resulting in the following linear regression equations between the Be(M) and SUS(M).

$$\text{Luochuan: } \mathrm{Be(M)_e} = 1.2431 \times \mathrm{SUS(M)} + 105.14 \quad (1)$$

$$\text{Xifeng: } \mathrm{Be(M)_e} = 1.2276 \times \mathrm{SUS(M)} + 79.689 \quad (2)$$

Where the estimated values $\mathrm{Be(M)_e}$ in Equations 1 and 2 are determined by the subtraction of the estimated climatic contribution (dust source and local precipitation) under the past 130-kyr average ^{10}Be production rate (Zhou et al. 2007b).

RESULTS AND DISCUSSION

Derived Relative ^{10}Be Production Rate Variation and Geomagnetic Excursion Events Records

After removal of the climate-contributed ^{10}Be, a residual signal ΔBe(ΔGM) is obtained by subtracting the estimated values ($\mathrm{Be(M)_e}$) from the measured Be(M) in 2 sites. The resulting residual signal is the amount of the ^{10}Be concentration modulated by geomagnetic intensity variations. The ΔBe(ΔGM) signal can then be normalized and scaled to 1 for the present for deriving the global relative ^{10}Be production rates variations (Figure 3a,b). It must be noted that Luochuan and Xifeng are located at about 35°N, where the latitudinal average production rate is about 0.0147 (atoms/cm^2 s) (Masarik and Beer 1999), similar to the global average of 0.0184 atoms/cm^2/s. Therefore, the separated geomagnetic modulated ^{10}Be signals can reliably reflect the global average ^{10}Be production rate variations.

Finally, we convert the normalized ^{10}Be production rate to the relative paleointensity using the formulas for ^{10}Be production rate and geomagnetic intensity reported by Xian et al. (2008), with the assumption that long-period ^{10}Be production rate fluctuations are mainly modulated by geomagnetic field (Masarik and Beer 1999). We can thus stack records into a composite relative paleointensity record for in-depth correlation analysis.

The plot of the 130-kyr residual ΔBe(ΔGM) signal and the stacked relative geomagnetic intensity record from Luochuan and Xifeng (Figure 3) clearly reveal the Laschamp and Blake events. The Laschamp event lies in the middle layer of L_1SS_1 (Figure 2), corresponding to the middle of MIS 3

https://doi.org/10.1017/S0033822200045082 Published online by Cambridge University Press

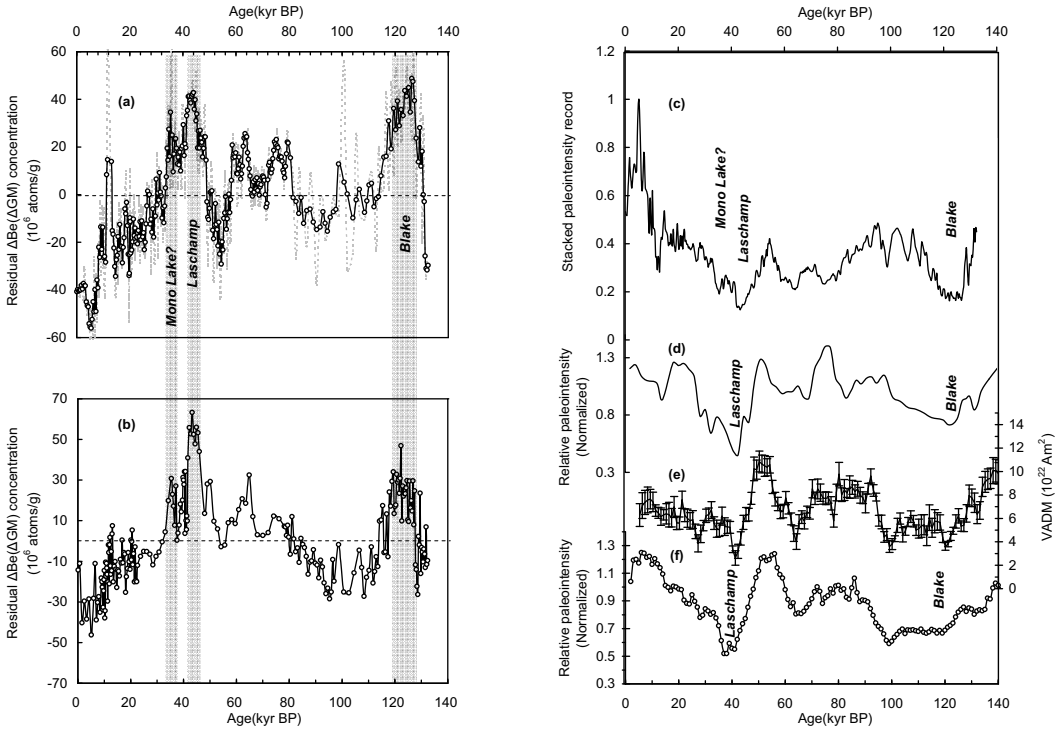

Figure 3 The reconstructed past 130-kyr geomagnetic excursion sequence from ^{10}Be in the (a) Luochuan and (b) Xifeng sections, and comparison of our stacked relative paleointensity result (c) with the records of (d) North Pacific (Yamazaki and Kanamatsu 2007), (e) PISO-1500 (Channell et al. 2009), and (f) SINT800 results (Guyodo and Valet 1999). Corresponding relative ^{10}Be production rates variations in (a) and (b) are labeled on the right coordinate, and time range and variation process of the excursions are depicted with the vertical bar.

at a depth of 492–524 cm in Luochuan and 584–620 cm in Xifeng. The age at this depth is about 43 kyr BP with duration of 3.9 kyr in 2 sections. The Blake event is located at the lower paleosol S_1 (S_1SS_3, Figure 2) at the depth of 1124–1176 cm in Luochuan and 1320–1424 cm in Xifeng. Its age is about 123 kyr BP with duration of 8.5 kyr in 2 sites. These 2 events coincide with periods of significant intensity drops and occur below a critical field less than 50% of the present-day field (Guyodo and Valet 1999). Reliable stratigraphic position of these 2 excursions determined by loess ^{10}Be also suggests the new time marker for future climatic correlations.

Geomagnetic Paleointensity Intercomparison

To check if our reconstructed paleointensity fits the global pattern, we compared our composite relative paleointensity result with those of the North Pacific (Figure 3d) (Yamanaki et al. 2007), the latest PISO-1500 (Figure 3e) record by Channell et al. (2009) who stacked many representative marine studies (e.g. Stoner et al. 2003; Carcaillet et al. 2004), and the SINT-800 curve (Figure 3f) (Guyodo and Valet 1999). All curves exhibit a similar low-frequency trend and each excursion event is characterized by a rapid start and termination, though its features are offset because of the different age model (Figure 3). The 4 curves clearly show the Blake and Laschamp geomagnetic minima at about 123 and 43 kyr BP, respectively, and with a smaller local minima at about 60–65 kyr BP. Our results also show the long rise in geomagnetic intensity common to most records observed between 40 and 5 kyr BP and a drop in intensity (reflected by an increased ^{10}Be production rate in Figure 3a and 3b)

https://doi.org/10.1017/S0033822200045082 Published online by Cambridge University Press

at about 35 kyr BP. However, we are not sure whether this dip at ~35 kyr BP corresponds to the Mono Lake event (Wagner et al. 2000), because the intensity peak is relatively small and is not obvious in some of the comparable records (Figure 3e and 3f).

The Blake and Laschamp events can apparently be extracted from the Luochuan and Xifeng sections, showing that these short-lived excursions may be well preserved in the loess-paleosol sequence even east of the Liupan Mountains (Figure 1). However, the climate-controlled pedogenesis, and dust accumulation effects have influenced the physical and chemical processes of ferromagnetic minerals in different paleosol and/or loess units. These processes lead to ambiguity in the geomagnetic excursion signal in some stratigraphic levels, which is hard to detect by paleomagnetic measurement (Zhu et al. 1998). As a result, it has been unclear in the past if there was a record of the Blake event in the loess-paleosol sequence (Zheng et al. 1995; Fang et al. 1997; Zhu et al. 1994, 1998; Pan et al. 2002). Our deconvolved atmospheric ^{10}Be production rate record shown here suggests that ^{10}Be in loess may directly reflect geomagnetic effects.

SUMMARY AND DISCUSSION

Results presented in this study suggest that loess-paleosol ^{10}Be records can indeed be used for geomagnetic field reconstruction once the remobilized dust and precipitation signal contamination are removed. The good agreement between our paleointensity records and comparison marine data sets spanning the last 130 kyr further indicates that our technique and analysis methods are indeed robust. Therefore, they could potentially be used to generate an extremely long record of geomagnetic intensities from Chinese loess-paleosol sequence, perhaps over the last 2.6 Myr.

ACKNOWLEDGMENTS

This work was jointly supported by the MOST special fund for State Key Laboratory of Loess and Quaternary Geology, Key Innovation project of the Chinese Academy of Sciences, National Science Foundations of China, the Ministry of Science and Technology of China, and the West Light Project of the Chinese Academy of Sciences. Measurements done at the NSF-Arizona AMS Laboratory were supported in part by NSF grant EAR06-22305, as well as AMS laboratory funds, and the work at Vienna was supported by VERA laboratory funds. We thank the anonymous reviewers and the editors for helpful comments and suggestions.

REFERENCES

An ZS, Sun DH. 1995. *Discussion on the Monsoon Variation over the Loess Plateau in the Last Glacial Cycle, in China Contribution to Global Change*. China: Beijing Science Press. 122 p.

An ZS, Liu TS, Lu YC, Porter SC, Kukla G, Wu XH, Hua YM. 1990. The long-term paleomonsoon variation recorded by the loess-paleosol sequence in central China. *Quaternary International* 7–8:91–5.

An ZS, Kukla G, Porter SC, Xiao JL. 1991. Magnetic susceptibility evidence of Monsoon variation on the Loess Plateau of central China during the last 130,000 years. *Quaternary Research* 36:29–36.

Beer J, Shen C, Heller F, Liu T, Bonani G, Beate D, Suter M, Kubik PW. 1993. ^{10}Be and magnetic susceptibility in Chinese loess. *Geophysical Research Letters* 20(1): 57–60.

Carcaillet JT, Bourlès DL, Thouveny N. 2004. Geomagnetic dipole moment and ^{10}Be production rate intercalibration from authigenic ^{10}Be/^{9}Be for the last 1.3 Ma. *Geochemistry, Geophysics, Geosystems* 5: Q05006, doi:10.1029/2003GC000641.

Channell JET, Xuan C, Hodell DA. 2009. Stacking paleointensity and oxygen isotope data for the last 1.5 Myr (PISO-1500). *Earth and Planetary Science Letters* 283(1–4):14–23.

Evans ME, Heller F. 2001. Magnetism of loess/palaeosol sequences: recent developments. *Earth-Science Reviews* 54(1–3):129–44.

Fang XM, Li JJ, Van der Voo R, Niocaill CM, Dai XR, Kemp RA, Derbyshire E, Cao JX, Wang JM, Wang G. 1997. A record of the Blake Event during the last interglacial paleosol in the western Loess Plateau of China. *Earth and Planetary Science Letters* 146(1–2): 73–82.

https://doi.org/10.1017/S0033822200045082 Published online by Cambridge University Press

Frank M, Schwarz B, Baumann S, Kubik PW, Suter M, Mangini A. 1997. A 200 kyr record of cosmogenic radionuclide production rate and geomagnetic field intensity from ^{10}Be in globally stacked deep-sea sediments. *Earth and Planetary Science Letters* 149(1–4): 121–9.

Gu ZY, Lal D, Liu TS, Southon J, Caffee MW, Guo ZT, Chen MY. 1996. Five million year ^{10}Be record in Chinese loess and red-clay: climate and weathering relationships. *Earth and Planetary Science Letters* 144(1–2):273–87.

Guyodo Y, Valet J-P. 1999. Global changes in intensity of the Earth's magnetic field during the past 800 kyr. *Nature* 399(6733):249–52.

Heller F, Shen CD, Beer J, Liu XM, Liu TS, Bronger A, Suter M, Bonani G. 1993. Quantitative estimates of pedogenic ferromagnetic mineral formation in Chinese loess and palaeoclimatic implications. *Earth and Planetary Science Letters* 114(2–3):385–90.

Johnsen SJ, Dahl-Jensen D, Gundestrup N, Steffensen JP, Clausen HB, Miller H, Masson-Delmotte V, Sveinbjörnsdóttir AE, White J. 2001. Oxygen isotope and palaeotemperature records from six Greenland ice-core stations: Camp Century, Dye-3, GRIP, GISP2, Renland and NorthGRIP. *Journal of Quaternary Science* 16(4):299–307.

Kukla G, An ZS. 1989. Loess stratigraphy in Central China. *Palaeogeography, Palaeoclimatology, Palaeoecology* 72(1–2):203–25.

Lu YC, Wang XL, Wintle AG. 2007. A new OSL chronology for dust accumulation in the last 130,000 years for the Chinese Loess Plateau. *Quaternary Research* 67(1):152–60.

Maher BA, Thompson R. 1988. Formation of ultrafine-grained magnetite in soils. *Nature* 336(6197):368–70.

Maher BA, Thompson R, Zhou LP. 1994. Spatial and temporal reconstructions of changes in the Asian palaeomonsoon: a new mineral magnetic approach. *Earth and Planetary Science Letters* 125(1–4):461–71.

Maher BA, Thompson R. 1995. Paleorainfall reconstructions from pedogenic magnetic susceptibility variations in the Chinese loess and paleosols. *Quaternary Research* 44(3):383–91.

Masarik J, Beer J. 1999. Simulation of particle fluxes and cosmogenic nuclide production in the Earth's atmosphere. *Journal of Geophysical Research* 104(D10): 12,099–11.

Muscheler R, Beer J, Kubik PW, Synal H-A. 2005. Geomagnetic field intensity during the last 60,000 years based on ^{10}Be and ^{36}Cl from the Summit ice cores and ^{14}C. *Quaternary Science Reviews* 24(16–17):1849–60.

Pan YX, Zhu RX, Liu QS, Guo B, Yue LP, Wu HN. 2002. Geomagnetic episodes of the last 1.2 Myr recorded in Chinese loess. *Geophysical Research Letters* 29(8): 1231–4.

Porter SC, An ZS. 1995. Correlation between climate events in the North Atlantic and China during the last glaciation. *Nature* 375(6529):305–8.

Porter SC, Hallet B, Wu XH, An ZS. 2001. Dependence of near-surface magnetic susceptibility on dust accumulation rate and precipitation on the Chinese Loess Plateau. *Quaternary Research* 55(3):271–83.

Shen CD, Beer J, Liu TS, Oeschger H, Bonani G, Suter M, Wölfli W. 1992. ^{10}Be in Chinese loess. *Earth and Planetary Science Letters* 109(1–2):169–77.

Stoner JS, Channell JET, Hodell DA, Charles CD. 2003. A 580 kyr paleomagnetic record from the sub-Antarctic South Atlantic (Ocean Drilling Program Site 1089). *Journal of Geophysical Research* 108(B5): 2244, doi:10.1029/2001JB001390.

Wagner G, Beer J, Laj C, Kissel C, Masarik J, Muscheler R, Synal H-A. 2000. Chlorine-36 evidence for the Mono Lake event in the Summit GRIP ice core. *Earth and Planetary Science Letters* 181(1–2):1–6.

Wang YJ, Cheng H, Edwards RL, An ZS, Wu JY, Shen CC, Dorale JA. 2001. A high-resolution absolute-dated Late Pleistocene monsoon record from Hulu Cave, China. *Science* 294(5550):2345–8.

Wu ZK. 2004. High-resolution ^{10}Be record from the middle part of the Loess Plateau, and the reconstruction of East Asian Monsoon history over the last 130 kyr [PhD dissertation]. Beijing: Graduate University of Chinese Academy of Sciences.

Xian F, An ZS, Wu ZK, Beck JW, Yu HG, Kang ZH, Cheng P. 2008. A simple model for reconstructing geomagnetic field intensity with ^{10}Be production rate and its application in Loess studies. *Science in China Series D* 51(6):855–61.

Yamazaki T, Kanamatsu T. 2007. A relative paleointensity record of the geomagnetic field since 1.6 Ma from the North Pacific. *Earth, Planets and Space* 59(7): 785–94.

Yuan DX, Cheng H, Edwards RL, Dykoski CA, Kelly MJ, Zhang ML, Qing JM, Lin YS, Wang YJ, Wu JY, Dorale JA, An ZS, Cai YJ. 2004. Timing, duration, and transitions of the Last Interglacial Asian Monsoon. *Science* 304(5670):575–8.

Zheng HB, Rolph T, Shaw J, An ZS. 1995. A detailed palaeomagnetic record for the last interglacial period. *Earth and Planetary Science Letters* 133(3–4):339–51.

Zhou LP, Oldfield F, Wintle AG, Robinson SG, Wang JT. 1990. Partly pedogenic origin of magnetic variations in Chinese loess. *Nature* 346(6286):737–9.

Zhou WJ, Priller A, Beck JW, Wu ZK, Chen MB, An ZS, Kutschera W, Xian F, Yu HG, Liu L. 2007a. Disentangling geomagnetic and precipitation signals in an 80-kyr Chinese loess record of ^{10}Be. *Radiocarbon* 49(1): 139–60.

Zhou WJ, Chen MB, Xian F, Song SH, Wu ZK, Jull AJT, Liu WG. 2007b. The mean value concept in mono-linear regression of multi-variables and its application to

https://doi.org/10.1017/S0033822200045082 Published online by Cambridge University Press

trace studies in geosciences. *Science in China Series D* 50(12):1828–34.

Zhu RX, Zhou LP, Laj C, Mazaud A, Ding ZL. 1994. The Blake geomagnetic polarity episode recorded in Chinese loess. *Geophysical Research Letters* 21(8):697–700.

Zhu RX, Coe RS, Guo B, Anderson R, Zhao XX. 1998. Inconsistent paleomagnetic recording of the Blake event in Chinese loess related to sedimentary environment. *Geophysical Journal International* 134(3):867–75.

Zhu RX, Zhang R, Deng CL, Pan YX, Liu QS, Sun YB. 2007. Are Chinese loess deposits essentially continuous? *Geophysical Research Letters* 34: L17306. doi: 10.1029/2007GL030591.

APPENDIX

Table 1 Luochuan results.

Depth (cm)	Age (kyr BP)	^{10}Be concentration (Be(M)) (10^6 atoms/g) (decay corrected)	Magnetic susceptibility (SUS(M)) (10^{-8} m^3/kg)
1	0.09	213.3	120.0
4	0.36	212.1	118.5
8	0.73	215.1	119.0
12	1.09	209.5	118.5
16	1.45	212.7	118.5
20	1.82	218.2	121.0
24	2.18	218.5	121.0
28	2.54	212.3	122.0
32	2.91	230.8	125.5
36	3.27	221.2	125.5
40	3.64	219.8	128.0
44	4.00	217.3	131.0
48	4.36	223.5	131.0
52	4.73	222.5	131.5
56	5.09	192.3	128.0
60	5.45	210.8	124.0
64	5.82	211.6	124.0
68	6.18	197.0	123.0
72	6.54	238.0	128.0
76	6.91	211.5	134.0
80	7.27	241.1	136.0
84	7.63	236.6	149.0
88	8.00	293.9	168.5
92	8.36	269.2	166.5
96	8.73	311.4	168.0
100	9.09	276.1	164.5
104	9.45	295.8	157.0
108	9.82	270.1	157.5
112	10.18	267.2	135.0
116	10.54	228.3	133.5
120	10.91	230.5	124.5
124	11.27	235.3	115.0
128	11.63	298.0	101.0

https://doi.org/10.1017/S0033822200045082 Published online by Cambridge University Press

Table 1 Luochuan results. *(Continued)*

Depth (cm)	Age (kyr BP)	^{10}Be concentration (Be(M)) (10^6 atoms/g) (decay corrected)	Magnetic susceptibility (SUS(M)) (10^{-8} m^3/kg)
132	13.07	229.6	108.5
136	13.39	224.2	108.0
140	13.71	226.3	113.5
144	14.03	186.8	77.5
148	14.35	166.9	76.0
152	14.67	154.0	74.0
156	14.99	168.2	72.5
160	15.30	180.3	70.0
164	15.62	168.3	81.0
168	15.94	188.0	69.5
172	16.26	167.2	72.5
176	16.58	194.3	76.5
180	16.90	169.4	76.5
184	17.22	164.2	70.5
188	17.53	168.3	72.0
192	17.85	185.0	73.5
196	18.17	177.6	71.5
200	18.49	198.4	67.0
204	18.81	161.6	59.5
208	19.13	169.5	53.5
212	19.45	153.6	54.5
216	19.77	164.7	91.0
217	19.84	191.1	92.5
218	19.92	186.9	79.0
219	20.00	158.5	67.0
220	20.08	190.4	60.0
221	20.16	163.5	55.0
224	20.40	129.0	47.0
228	20.72	137.2	49.0
232	21.04	162.8	51.5
236	21.36	144.8	51.5
240	21.68	169.1	51.5
244	22.00	149.4	57.5
248	22.31	155.5	52.5
252	22.63	147.1	48.0
256	22.95	146.3	50.0
260	23.27	155.1	59.0
264	23.59	175.2	57.0
268	23.91	146.0	56.0
272	24.23	170.3	56.0
276	24.54	149.4	54.5
280	24.86	177.1	62.0
284	25.18	151.5	57.0
288	25.50	162.6	61.0
292	25.82	157.5	63.5
296	26.14	171.0	65.0

https://doi.org/10.1017/S0033822200045082 Published online by Cambridge University Press

Table 1 Luochuan results. *(Continued)*

Depth (cm)	Age (kyr BP)	^{10}Be concentration (Be(M)) (10^6 atoms/g) (decay corrected)	Magnetic susceptibility (SUS(M)) (10^{-8} m^3/kg)
300	26.46	191.9	66.0
304	26.78	184.5	67.0
308	27.09	202.6	75.5
312	27.41	200.8	77.0
316	27.73	197.2	77.0
320	28.05	168.1	77.5
324	28.37	208.1	78.0
328	28.69	186.0	81.0
332	29.01	202.2	81.5
336	29.32	178.3	82.5
340	29.64	213.6	82.5
344	29.96	201.7	80.5
348	30.28	224.1	82.0
352	30.60	182.4	83.5
356	30.92	221.5	84.5
360	31.24	218.5	84.5
364	31.55	220.8	86.5
368	31.87	200.0	87.0
372	32.19	217.4	87.5
376	32.51	195.4	88.5
380	32.83	217.4	90.5
384	33.15	205.3	93.0
388	33.47	220.0	91.5
392	33.79	244.1	93.5
396	34.10	224.9	97.5
400	34.42	266.6	100.0
404	34.74	234.0	97.5
408	35.06	263.8	97.5
412	35.38	231.3	99.0
416	35.70	293.2	100.5
420	36.02	239.7	101.5
424	36.33	237.8	104.0
428	36.65	246.4	100.0
432	36.97	262.7	102.0
436	37.29	259.9	107.0
440	37.61	257.4	108.0
444	37.93	258.7	108.5
448	38.25	240.3	107.0
452	38.57	265.0	107.5
456	38.88	246.8	106.5
460	39.20	255.0	106.0
464	39.52	238.4	105.0
468	39.84	275.6	107.0
472	40.16	259.3	107.0
476	40.48	268.3	107.5
480	40.80	236.7	107.0

https://doi.org/10.1017/S0033822200045082 Published online by Cambridge University Press

Table 1 Luochuan results. *(Continued)*

Depth (cm)	Age (kyr BP)	^{10}Be concentration (Be(M)) (10^6 atoms/g) (decay corrected)	Magnetic susceptibility (SUS(M)) (10^{-8} m^3/kg)
484	41.11	275.9	108.5
488	41.43	263.6	107.5
492	41.75	276.1	106.5
496	42.07	279.0	105.5
500	42.39	278.4	105.5
504	42.71	277.4	107.0
508	43.03	273.6	105.5
512	43.34	276.4	106.5
516	43.66	284.5	106.0
520	43.98	273.7	103.5
524	44.30	276.7	105.0
528	44.62	264.8	107.0
532	44.94	288.1	105.5
536	45.26	252.7	107.0
540	45.58	272.1	106.0
544	45.89	245.4	105.5
548	46.21	274.1	107.0
552	46.53	251.8	107.0
556	46.85	271.2	108.5
560	47.17	265.8	108.0
564	47.49	246.9	107.5
568	47.81	254.8	110.0
572	48.12	278.0	109.0
576	48.44	263.9	109.5
580	48.76	255.3	110.5
584	49.08	250.5	110.5
588	49.40	202.9	102.5
592	49.72	224.6	101.5
596	50.04	251.1	113.5
600	50.35	233.3	115.5
604	50.67	268.2	120.5
608	50.99	267.7	126.0
612	51.31	257.2	134.0
616	51.63	224.2	125.0
620	51.95	257.2	126.0
624	52.27	270.6	131.0
628	52.59	264.3	135.5
632	52.90	246.5	138.5
636	53.22	272.1	137.5
640	53.54	244.4	136.0
644	53.86	278.7	140.5
648	54.18	234.1	139.0
652	54.50	255.4	132.0
656	54.82	238.9	131.5
660	55.13	243.3	124.0
664	55.45	236.0	124.5

https://doi.org/10.1017/S0033822200045082 Published online by Cambridge University Press

Table 1 Luochuan results. *(Continued)*

Depth (cm)	Age (kyr BP)	^{10}Be concentration (Be(M)) (10^6 atoms/g) (decay corrected)	Magnetic susceptibility (SUS(M)) (10^{-8} m^3/kg)
668	55.77	258.1	115.0
672	56.09	234.7	111.5
676	56.41	243.1	113.5
680	56.73	214.1	113.0
684	57.05	244.2	108.5
688	57.37	243.6	107.5
692	57.68	231.0	108.0
696	58.00	221.0	108.5
700	58.32	248.2	98.0
704	58.64	231.0	88.5
708	58.96	233.6	83.0
712	59.28	198.6	71.0
716	59.60	203.6	62.5
720	59.91	204.4	62.5
724	60.23	191.2	61.0
728	60.55	173.6	59.0
732	60.87	197.4	57.5
736	61.19	189.6	54.5
740	61.51	183.8	55.5
744	61.83	183.1	53.5
748	62.14	170.9	54.0
752	62.46	186.4	52.5
756	62.78	192.1	53.0
760	63.10	194.1	52.5
764	63.42	199.3	54.5
768	63.74	195.7	51.5
772	64.06	189.0	52.0
776	64.38	194.4	50.0
780	64.69	171.2	48.0
784	65.01	173.9	46.5
788	65.33	175.6	44.5
792	65.65	160.9	47.0
796	65.97	151.9	42.5
800	66.29	167.3	43.0
804	66.61	154.0	43.0
808	66.92	171.2	43.5
812	67.24	155.6	44.0
816	67.56	170.4	43.5
820	67.88	157.5	42.0
824	68.20	167.8	42.5
828	68.52	153.1	42.5
832	68.84	165.5	41.5
836	69.15	153.3	42.5
840	69.47	167.2	45.5
844	69.79	176.6	48.0
848	70.11	169.0	48.0

https://doi.org/10.1017/S0033822200045082 Published online by Cambridge University Press

Table 1 Luochuan results. *(Continued)*

Depth (cm)	Age (kyr BP)	^{10}Be concentration (Be(M)) (10^6 atoms/g) (decay corrected)	Magnetic susceptibility (SUS(M)) (10^{-8} m^3/kg)
852	70.43	173.5	49.0
856	70.75	181.3	53.0
860	71.07	167.6	50.0
864	71.39	161.7	54.0
868	71.70	179.4	64.0
872	72.02	197.6	70.5
876	72.34	214.5	72.5
880	72.66	210.2	74.0
884	72.98	203.0	72.0
888	73.30	201.3	71.5
892	73.62	206.2	72.0
896	73.93	206.5	71.0
900	74.25	210.3	68.0
904	74.57	204.1	62.0
908	74.89	198.0	55.5
912	75.21	188.8	53.0
916	75.53	202.5	56.0
920	75.85	180.7	48.0
924	76.17	180.2	48.0
928	76.48	179.8	49.0
932	76.80	178.5	43.5
936	77.12	167.1	38.5
940	77.44	165.8	37.5
944	77.76	170.2	41.0
948	78.08	166.1	47.0
952	78.40	176.9	49.0
956	78.71	177.7	52.0
960	79.03	187.9	53.0
964	79.35	202.5	57.0
968	79.67	215.6	70.5
972	80.55	322.2	162.0
976	81.55	362.2	200.5
980	82.63	338.4	209.5
984	83.73	360.9	197.0
988	84.55	297.9	161.0
992	85.51	363.4	213.5
996	86.68	355.6	219.0
1000	87.93	379.9	214.0
1004	89.13	358.5	208.0
1008	90.46	325.6	208.0
1012	91.74	353.7	200.5
1016	92.78	356.7	204.0
1020	93.63	344.2	207.5
1024	94.47	325.5	189.5
1028	95.52	375.4	227.0
1032	96.71	349.2	197.5

https://doi.org/10.1017/S0033822200045082 Published online by Cambridge University Press

Table 1 Luochuan results. *(Continued)*

Depth (cm)	Age (kyr BP)	^{10}Be concentration (Be(M)) (10^6 atoms/g) (decay corrected)	Magnetic susceptibility (SUS(M)) (10^{-8} m^3/kg)
1036	97.67	377.1	225.5
1040	98.68	382.8	230.5
1048	100.77	455.5	237.0
1052	101.97	373.6	241.0
1060	104.08	364.8	228.0
1064	105.35	427.8	239.0
1068	106.52	385.2	232.0
1076	108.49	392.9	240.0
1080	109.31	398.8	239.0
1084	110.18	405.9	237.0
1088	111.12	409.9	237.5
1092	112.05	394.6	234.0
1096	112.90	380.7	240.5
1100	113.73	421.4	238.5
1104	114.66	403.3	239.0
1108	115.73	388.2	225.5
1112	116.59	422.5	220.5
1116	117.53	388.1	226.0
1120	118.53	431.7	224.5
1124	119.45	385.4	219.0
1128	120.21	418.0	209.0
1132	120.87	379.9	204.5
1136	121.54	386.1	190.5
1140	122.26	357.9	185.5
1144	122.99	374.6	184.0
1148	123.66	357.5	173.5
1152	124.33	395.5	190.5
1156	125.08	367.3	184.0
1160	125.73	352.9	161.0
1164	126.24	300.3	138.5
1168	126.74	343.6	131.0
1172	127.29	343.1	156.0
1176	127.92	314.6	169.5
1180	128.76	332.2	160.0
1184	129.30	246.2	102.0
1188	129.72	204.2	46.0
1192	130.16	153.8	55.5
1196	130.58	220.7	66.5
1200	130.95	149.0	45.5
1204	131.29	111.6	28.5
1208	131.66	103.8	27.5
1212	132.05	111.5	28.0
1216	132.39	109.0	28.0

https://doi.org/10.1017/S0033822200045082 Published online by Cambridge University Press

Table 2 Xifeng results.

Depth (cm)	Age (kyr BP)	^{10}Be concentration (Be(M)) (10^6 atoms/g) (decay corrected)	Magnetic susceptibility (SUS(M)) (10^{-8} m^3/kg)
1	0.11	179.5	93.0
4	0.66	176.0	87.5
8	1.55	146.8	87.5
12	2.43	157.8	87.8
16	3.31	150.8	89.3
20	4.19	157.0	86.3
24	5.08	141.2	87.8
28	5.96	159.8	88.3
32	6.53	189.8	98.8
36	7.01	170.0	105.3
40	7.48	189.4	114.0
44	7.95	210.0	128.5
48	8.43	207.2	132.5
52	8.90	224.8	133.0
56	9.12	218.6	129.5
60	9.27	212.8	127.0
64	9.43	191.7	118.8
68	9.58	189.1	115.8
72	9.73	187.1	107.5
76	9.89	193.5	108.3
80	10.04	181.7	95.0
84	10.19	165.5	100.8
88	10.34	153.9	88.5
92	10.50	172.3	84.0
96	10.65	164.8	83.5
100	10.80	168.7	81.5
104	10.96	163.3	79.0
108	11.11	163.9	82.0
112	11.26	148.9	80.5
116	11.42	125.8	54.0
120	11.57	141.0	51.5
124	11.72	164.8	74.0
128	11.88	183.8	102.0
132	12.03	222.1	117.5
140	12.18	168.0	70.5
144	12.33	131.3	52.0
148	12.49	124.0	49.5
152	12.64	146.3	58.5
156	12.79	136.3	58.0
160	12.95	153.8	57.5
164	13.10	145.5	47.5
168	13.43	122.2	51.0
172	13.76	118.1	41.5
176	14.10	124.8	45.0
180	14.43	122.9	46.5
184	14.76	108.4	42.0

https://doi.org/10.1017/S0033822200045082 Published online by Cambridge University Press

Table 2 Xifeng results. *(Continued)*

Depth (cm)	Age (kyr BP)	^{10}Be concentration (Be(M)) (10^6 atoms/g) (decay corrected)	Magnetic susceptibility (SUS(M)) (10^{-8} m^3/kg)
188	15.09	112.8	38.5
192	15.43	115.1	41.0
196	15.76	112.7	41.0
200	16.09	120.3	40.5
204	16.42	116.7	39.0
208	16.76	129.9	40.5
212	17.09	116.9	39.0
216	17.42	121.9	39.0
220	17.75	122.4	40.0
224	18.09	104.1	40.5
228	18.42	111.2	40.0
232	18.75	120.1	44.0
236	19.08	119.4	37.0
240	19.42	119.2	40.5
244	19.75	120.4	44.5
260	20.08	132.4	42.5
264	20.26	123.1	43.0
268	20.44	129.7	41.0
272	20.61	134.7	40.5
276	20.79	117.7	40.5
280	21.09	123.1	40.5
284	21.39	109.9	41.0
288	21.69	126.5	40.5
292	21.99	110.5	41.0
296	22.29	111.8	42.5
300	22.59	119.3	42.0
320	23.75	124.3	42.5
340	24.92	129.2	44.5
360	26.08	137.7	51.5
380	27.25	142.6	56.5
400	28.41	135.5	55.0
420	29.58	145.1	59.5
440	30.74	146.0	58.5
460	31.91	159.7	65.5
480	33.07	167.1	67.5
488	34.24	191.6	75.0
492	35.40	206.8	78.5
496	35.82	198.4	78.0
500	36.24	195.1	80.0
504	36.66	187.5	81.5
508	37.08	204.4	79.5
512	37.51	174.0	76.5
516	37.93	181.8	80.0
520	38.35	183.3	78.0
524	38.77	194.2	78.5
528	39.19	187.4	76.0

https://doi.org/10.1017/S0033822200045082 Published online by Cambridge University Press

Table 2 Xifeng results. *(Continued)*

Depth (cm)	Age (kyr BP)	^{10}Be concentration (Be(M)) (10^6 atoms/g) (decay corrected)	Magnetic susceptibility (SUS(M)) (10^{-8} m^3/kg)
536	39.61	196.8	79.0
540	39.80	207.3	78.5
544	39.98	204.8	77.5
548	40.17	200.2	75.5
552	40.35	204.7	74.0
556	40.54	175.5	75.0
560	40.72	204.1	73.5
564	40.91	178.1	72.0
568	41.09	174.3	72.5
572	41.28	177.4	69.5
576	41.46	177.3	71.5
580	41.65	206.5	70.0
584	42.19	219.0	68.0
588	42.74	214.1	66.5
592	43.28	221.5	64.0
600	43.83	213.1	66.0
620	44.37	215.3	71.5
640	44.91	219.8	68.5
660	45.46	214.0	66.0
680	46.00	207.8	68.5
700	47.98	171.9	64.0
720	49.00	182.7	61.0
740	50.12	188.1	64.5
760	51.50	195.0	86.0
780	52.88	201.6	94.5
800	54.25	207.6	106.5
820	55.58	197.3	97.5
840	56.91	194.8	86.5
860	58.24	184.1	76.5
880	59.57	179.7	74.5
900	60.90	155.9	49.5
920	62.23	154.4	44.0
940	63.57	149.2	41.5
960	64.90	155.1	35.0
980	66.23	131.0	32.0
1000	67.98	123.2	33.0
1020	70.02	122.9	33.0
1040	72.06	130.4	38.0
1060	74.09	142.9	41.5
1080	76.13	145.3	44.5
1100	78.17	135.4	39.5
1104	78.58	128.9	34.5
1108	78.98	138.9	46.0
1112	79.39	158.0	57.5
1116	79.80	158.9	63.0
1120	80.41	232.1	129.5

https://doi.org/10.1017/S0033822200045082 Published online by Cambridge University Press

Table 2 Xifeng results. *(Continued)*

Depth (cm)	Age (kyr BP)	^{10}Be concentration (Be(M)) (10^6 atoms/g) (decay corrected)	Magnetic susceptibility (SUS(M)) (10^{-8} m^3/kg)
1124	81.08	240.2	121.0
1128	81.76	258.7	145.0
1132	82.43	253.0	145.5
1136	83.11	254.9	145.5
1140	83.78	250.2	147.5
1144	84.46	251.6	139.0
1148	85.13	257.9	146.5
1152	85.81	253.8	144.5
1156	86.48	239.7	136.5
1160	87.16	245.0	148.0
1164	87.83	242.3	141.0
1168	88.51	248.6	145.5
1172	89.18	246.0	139.0
1176	89.86	249.2	147.0
1180	90.53	266.8	162.0
1184	91.21	258.0	160.0
1188	91.88	266.6	160.0
1192	92.56	270.7	166.0
1196	93.23	271.5	173.0
1200	93.91	280.8	185.0
1204	94.58	286.7	187.5
1208	95.26	287.5	192.5
1212	95.93	295.8	196.5
1216	96.47	303.2	189.5
1220	96.97	288.2	186.0
1224	98.67	296.4	178.0
1228	100.63	303.7	203.0
1232	102.59	307.1	206.0
1236	104.54	305.2	196.5
1240	106.50	318.8	198.5
1244	107.42	279.6	173.5
1248	108.34	293.7	196.5
1252	109.27	287.7	184.0
1256	110.19	291.1	184.0
1260	111.11	300.8	182.5
1264	111.72	300.2	196.5
1268	112.34	303.4	194.5
1272	112.95	303.4	188.5
1276	113.56	297.9	188.0
1280	114.17	314.1	183.0
1284	114.79	315.3	183.5
1288	115.40	326.6	187.0
1292	115.90	309.1	191.5
1296	116.40	318.6	199.0
1300	116.90	333.0	195.5
1304	117.40	302.1	187.5

https://doi.org/10.1017/S0033822200045082 Published online by Cambridge University Press

Table 2 Xifeng results. *(Continued)*

Depth (cm)	Age (kyr BP)	^{10}Be concentration (Be(M)) (10^6 atoms/g) (decay corrected)	Magnetic susceptibility (SUS(M)) (10^{-8} m^3/kg)
1308	117.90	334.6	188.0
1312	118.40	317.8	180.0
1316	118.90	328.8	179.0
1320	119.40	341.4	185.5
1324	119.72	316.0	181.5
1328	120.05	323.1	184.5
1332	120.37	319.6	181.0
1336	120.69	335.9	182.0
1340	121.02	343.7	191.5
1344	121.34	339.9	187.5
1348	121.66	328.4	183.5
1352	121.98	325.3	175.0
1356	122.31	338.4	172.5
1360	122.63	312.3	181.5
1364	122.95	327.8	180.0
1368	123.28	322.7	180.0
1372	123.60	320.3	177.0
1376	123.92	320.3	177.0
1380	124.25	336.0	187.5
1384	124.57	326.6	177.0
1388	124.89	316.5	184.5
1392	125.22	315.7	184.5
1396	125.54	312.4	165.5
1400	125.86	299.2	165.5
1404	126.18	285.5	151.5
1408	126.51	273.7	146.0
1412	126.83	298.4	154.0
1416	127.15	263.8	143.5
1420	127.48	274.4	138.5
1424	127.80	237.4	138.0
1428	128.09	225.9	130.5
1432	128.37	207.2	122.0
1436	128.66	201.9	121.0
1440	128.94	230.5	121.0
1444	129.23	235.5	128.5
1448	129.51	250.6	120.0
1452	129.80	196.2	108.0
1456	130.09	209.1	108.0
1460	130.37	209.9	110.5
1464	130.66	197.1	104.0
1468	130.94	199.1	100.5
1472	131.23	180.6	87.5
1476	131.51	180.8	93.0
1480	131.80	178.7	75.0
1484	132.09	171.3	84.0
1488	132.37	177.4	87.5

https://doi.org/10.1017/S0033822200045082 Published online by Cambridge University Press